XRD and NMR characterization of synthetic hectorites and the corresponding surfactant-exchanged clays

A. GERSTMANS[1], L. URBANCZYK[2], R. JÉRÔME[2], J.-L. ROBERT[3] AND J. GRANDJEAN[1],*

[1] *COSM, University of Liège, Institute of Chemistry B6a, Sart-Tilman, B-4000-Liège, Belgium,*
[2] *CERM, University of Liège, Institute of Chemistry B6a, Sart-Tilman, B-4000-Liège, Belgium, and*
[3] *IMPMC Campus Boucicaut, 140 rue de Lourmel, F-75015 Paris, France*

ABSTRACT: Synthetic hectorites and the corresponding surfactant-exchanged clays have been characterized by X-ray diffraction and ^{1}H, ^{7}Li, ^{13}C, ^{23}Na and ^{29}Si solid-state nuclear magnetic resonance (NMR) spectroscopy. The low-charge clays retain water more efficiently, forming aggregates without extensive drying. The hydroxylated hectorite exhibits two ^{1}H NMR signals near 0 ppm whereas the fluorohectorites are characterized by a single peak in the same region. The ^{23}Na 2D 3Q magic angle spinning (MAS) spectra of the low-charge hectorites show a single peak. The ^{29}Si NMR shift depends on the interlayer charge. Tactoids formed by the low-charge hectorites reduce the rate of surfactant incorporation. The population of the all-*trans* conformer of the hydrocarbon chain, determined by ^{13}C MASNMR, varies with the surfactant content. ^{13}C NMR relaxation data show an increase in mobility with the surfactant loading and along the long alkyl chain, from the polar head to the terminal group. Complexity of the motional behaviour precludes any detailed analysis. These modified clays are not useful in preparing poly(ε-caprolactone) nanocomposites by *in situ* polymerization.

One of the critical steps in the creation of polymer/clay nanocomposites is the surface treatment of the mineral. Cationic surfactants are ion-exchanged with interlamellar cations to form intercalated clay-surfactant hybrids. The surface treatment is to ensure the dispersion of the mineral within the polymer matrix. Such systems are currently characterized by macroscopic techniques such as X-ray diffraction (XRD), thermogravimetric analysis (TGA) or transmission electron microscopy (TEM). For instance, the d_{001} basal spacing calculated from XRD data may be indirectly related to the number of surfactant layer(s) and their mean orientation with respect to the clay basal plane (Lagaly, 1986). Nuclear magnetic resonance (NMR) spectroscopy complements XRD data at a molecular level, probing the structure, conformation and dynamics of the intercalated surfactant ions. Thus, the conformation change of the surfactant hydrocarbon chain can be monitored quantitatively (He *et al.*, 2004; Müller *et al.*, 2004). In contrast, molecular motions of the intercalated surfactants can be characterized by the NMR relaxation parameters (Kubies *et al.*, 2002; Hrobarikova *et al.*, 2004; Osman *et al.*, 2004; Mirau *et al.*, 2005; Urbanczyk *et al.*, 2006; Wen *et al.*, 2006; Borsacchi *et al.*, 2007). Previous NMR studies of clayey

materials have been summarized recently (Grandjean, 2006). Infrared (IR) spectroscopy (Vaia *et al.*, 1994; Li & Ishida, 2003) and molecular dynamics simulation (Heinz *et al.*, 2007) are also useful for characterizing such hybrid materials.

Our previous studies reported on Laponite, a commercial synthetic hectorite of small charge (Kubies *et al.*, 2002; Urbanczyk *et al.*, 2006), and also results obtained after modification of synthetic saponites of variable interlayer charge (Müller *et al.*, 2004; Hrobarikova *et al.*, 2004; Urbanczyk *et al.*, 2006). The synthetic hectorites were character-ized by XRD and NMR measurements. In particular, the Na counter-ion surrounding was investigated by two-dimensional 3 quantum magic angle spinning NMR (2D 3QMAS NMR) and compared with the results obtained from the synthetic saponites (Delevoye *et al.*, 2003). Previously, we prepared polymer/saponite nano-composites with reasonable yields, whereas Laponite-based nanocomposites were obtained with small yields at best (Hrobarikova *et al.*, 2004; Urbanczyck *et al.*, 2006). Since Laponite consists of small platelets, possibly leading to poorer polymer intercalation, we have investigated the ability of synthetic hectorites (prepared with the same equipment as the synthetic saponites) to form nanocomposites. The surfactant-exchanged hector-ites used for the formation of the nanocomposites are also characterized by XRD and NMR measure-ments, and compared with the exchanged saponites. The location of isomorphous substitutions, different for hectorite and saponite, could induce different interactions with the positively charged surfactant, changing the structure and/or dynamics of the intercalated species.

MATERIALS AND METHODS

Materials

The syntheses of the differently charged hector-ites were obtained from gels of appropriate compositions prepared according to the conven-tional gelling method (Hamilton & Henderson, 1968). Typically, Li_2CO_3 and Na_2CO_3 dried at 110ºC were added to a solution of $Mg(NO_3)_2$ with a few drops of nitric acid to complete the transforma-tion of carbonates. A similar volume of ethanol was poured into the aqueous solution and tetraethyl orthosilicate (TEOS) was added as the Si source.

The gel was then precipitated by adding NH_3. After hydrolysis was complete (~12 h), the gel was dried and calcined, and the temperature increased progressively to 600ºC, whereby the sample powdered. These variably charged hectorites were prepared by hydrothermal synthesis in Morey-type externally heated pressure vessels, internally coated with silver tubing, at 400ºC and 1 kbar pressure (H_2O), for a run duration of four weeks. To obtain the fluorohectorites, MgF_2, dried at 110ºC, was used instead of the $Mg(NO_3)_2$ solution. As the high-charge hectorites are unstable in the hydroxylated form, the clay with 0.40 charge per half unit cell was the only one obtained. The chemical formulae of the hectorites prepared were $Na_{0.4}(Mg_{2.6}Li_{0.4})$ $Si_4O_{10}(OH)_2.nH_2O$ (HecOH-0.40), $Na_{0.4}(Mg_{2.6}Li_{0.4})$ $Si_4O_{10}F_2.nH_2O$ (HecF-0.40) and $Na_{0.8}(Mg_{2.2}Li_{0.8})$ $Si_4O_{10}F_2.nH_2O$ (HecF-0.80). Before use, the clays were dried at 90ºC for at least 6 h and then equilibrated at room temperature. The hectorites were exchanged with hexadecyltrimethylammonium bromide (HDTA: $(CH_3)_3N^+(CH_2)_{15}CH_3$) (Scheme, Fig. 4), as described previously (Kubies *et al.*, 2002). The starting amount of HDTA was varied in order to obtain hybrid materials with different amounts of intercalated surfactant (Table 1).

XRD data

The XRD patterns of the samples were recorded at 25ºC using a Siemens D5000 powder diffract-ometer using Cu-$K\alpha$ radiation (λ = 1.54 Å) and a Ni filter.

TGA

The thermal analyses used to calculate the surfactant content of the hybrid materials were performed using a Thermal Analyst 2100 apparatus in the heating range 20−800ºC at a heating rate of 10ºC/min, under N_2 flow.

NMR spectra

The ^7Li, ^{23}Na and ^{29}Si MAS spectra, as well as ^{13}C cross-polarization (CP) MAS spectra, were recorded using 4 mm zirconia rotors spinning at 7 kHz in a Bruker Avance DSX 400WB spectro-meter (B_0 = 9.04 T) working at the Larmor frequency of 155.45, 105.95, 79.50 and 100.62 MHz, respectively. The ^{13}C, ^{23}Na, ^{29}Si and ^7Li chemical shifts were referenced relative to

TABLE 1. Main characteristics of the modified hectorites.

Starting composition	Exchange time (h)	d_{001} (Å)	d_{001} (Å)	HDTA content (CEC unit)
(A) 1.5 g HecF-0.80 + 1.5 g HDTA	80		30.5	0.85
(B) 1.5 g HecF-0.80 + 0.475 g HDTA	46		28.4	0.63
(C) 1.5 g HecF-0.80 + 0.240 g HDTA	44		28.0	0.36
(1) 1.5 g HecF-0.40 + 1.5 g HDTA	96		22.3	0.75
(4) 1 g de (3) + 1 g HDTA	48	44.1	19.7	0.69
(3) 1.5 g HecF-0.40 + 1.5 g HDTA	46	41.7	19.5	0.52
(2) 1.5 g HecF-0.40 + 0.375 g HDTA	48	38.1	17.2	0.45

TMS, NaCl (1 M), TMS, and LiOH (1 M), respectively. The ^{13}C CP MAS NMR spectra were performed under high-power proton decoupling (83 kHz) with a (relaxation) delay time of 4 s (>5 imes the relaxation times $T_{1\rho}(H)$), and a contact time of 2 ms. The quantitative spectra and time constants T_{CH} were determined from the plots of line intensity *vs.* contact time in the CP MAS experiments, as described previously (Müller *et al.*, 2004). These experiments (16 delays) were run with 3000 scans.

The ^{13}C NMR longitudinal relaxation times in the laboratory frame $T_1(C)$ and in the rotating frame $T_{1\rho}$ (C) were determined by application of the usual CP pulse sequences (^{13}C 90º pulse of 5.5 μs, relaxation delays of 6 s and 1 s, respectively; 15 delays − 4000 scans). The relaxation delay allows the spin system to reach its equilibrium value between two successive pulse sequences. The values used were >5 times the longest relaxation time.

The ^1H MAS NMR spectra were recorded at a spinning rate of 20 kHz with 2.5 mm zirconia rotors using single pulse experiments. The ^{23}Na 2D MQMAS NMR spectra were recorded with a three-pulse sequence (1.9, 0.9 and 9 μs), a Z-filter (Amoureux *et al.*, 1996) and a rotation-synchronized acquisition (at the rotor − 2.5 mm) spinning rate of 20 kHz.

IR spectra

The IR spectra were collected using a Perkin Elmer 16PC Fourier transform infrared (FTIR) spectrometer with a nominal resolution of 2 cm^{-1}. Spectra were obtained from KBr pellets, using four interferograms.

RESULTS AND DISCUSSION

Synthetic hectorites

The basal spacing values obtained for the clays HecOH-0.40 (d_{001} = 12.6 Å), HecF-0.40 (12.4 Å) and HecF-0.80 (12.2 Å) are similar to those of the synthetic saponites investigated previously (Müller *et al.*, 2004). However, an extra diffraction peak (26−27 Å) observed for the two low-charge hectorites, equilibrated at room temperature after drying at 90ºC, results from swelling due to residual water. This extra signal can be removed by drying at 150ºC for 24 h and also leads to a small decrease in the remaining d_{001} value (11.0 Å). The ^{29}Si MAS NMR spectrum of the three hectorites shows a single peak at −94.1 ppm (HecOH), −94.5 ppm (HecF-0.40) and −92.3 ppm (HecF-0.80). The charge effect is in line with a recent paper showing an increase in the chemical shift with the charge of micas and saponites (Sanz *et al.*, 2006). The ^7Li NMR signal occurs at −0.73 ppm (HecF-0.40 and HecF-0.80) and −0.33 ppm (HecOH-0.40). In addition to the water protons near 4 ppm, the structural hydroxyl groups of trioctahedral clays show a single ^1H NMR signal near 0.5 ppm (Alba *et al.*, 2000). HecOH-0.40 shows three peaks at 3.97, 0.33 and −0.42 ppm, respectively. Drying HecOH-0.40 at 150ºC for 24 h gives rise to a strong reduction of the signal at 3.97 ppm, assigned to water protons, but the two other signals of similar intensities (0.48 ppm and 0.52 ppm, respectively) remain unchanged. Chemical-shift distribution, resulting from heterogeneous orientation, could explain the greater line width of the signal at −0.42 ppm (362 Hz compared to 172 Hz of the 0.33 ppm peak).

However, the broader signal cannot be assigned to the hydroxyl groups at the edges of the (probably) small hectorite platelets. The hydroxyl groups of silica occur at greater (positive) chemical shifts (d'Espinose de la Caillerie *et al.*, 1997) and the ^{29}Si MAS NMR spectrum should show a significant (non-detected) signal at approximately -87 ppm, characteristic of the Q_2 units.

The ^{23}Na MAS NMR spectra of the three hectorites exhibit band shapes more complex than those observed previously in low-charge saponites (Delevoye *et al.*, 2003). Figure 1 shows a typical example. This behaviour suggests stronger second order effects that are not suppressed by MAS due to greater quadrupolar interaction. The 2D 3QMAS spectra are used to cancel such effects and estimate the strength of the quadrupolar interaction. The details of these experiments are described in the literature (Rocha *et al.*, 2003) and the relevant equations for ^{23}Na have been given previously (Delevoye *et al.*, 2003). For HecOH-0.40, the calculated isotropic chemical shift (-2.1 ppm) occurs in the chemical-shift range of the low-charge saponites (Delevoye *et al.*, 2003). The calculated quadrupolar product (2.9 MHz) is significantly greater than those obtained with the low-charge saponites (Delevoye *et al.*, 2003). Accordingly, the counter-ion surrounding is less symmetric in the hectorites than in the low-charge saponites. HecF-0.40 shows similar values (-2.5 ppm and 3.0 MHz).

Modified hectorites

The HDTA intercalation in HecF-0.80 provides a single basal spacing value (d_{001}) in the $28-30$ Å range (Table 1), associated with a paraffin-type
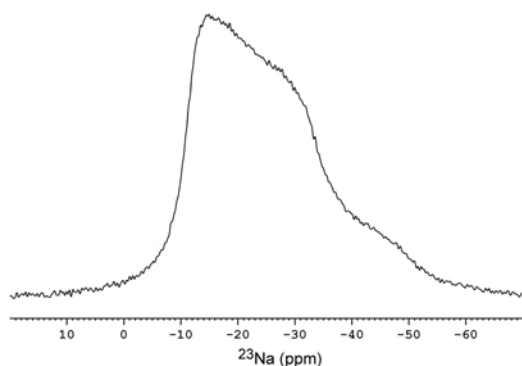

Fig. 1. ^{23}Na MAS spectrum of HecOH-0.40.

monolayer arrangement of the long hydrocarbon chains tilted at an angle of ~55º with respect to the basal plane (Lagaly, 1986). Similar values were obtained for HDTA-exchanged saponites of 0.75 and 0.80 charge per half unit cell (Müller *et al.*, 2004). A single major diffraction peak is also observed with all the previous modified clays of different charges (Kubies *et al.*, 2002; Hrobarikova *et al.*, 2004; Urbanczyk *et al.*, 2006). In contrast, both HDTA-HecF-0.40 and HDTA-HecOH-0.40 (not shown) exhibit a different pattern upon surfactant intercalation (Table 1). With the small surfactant contents, the smaller d_{001} values ($17.2-19.5$ Å) correspond to a lateral bilayer arrangement of the surfactant molecules with the long alkyl chains lying down on the clay surface (17.2 Å) or a pseudotrilayer arrangement (~19 Å) (Lagaly, 1986; Heinz *et al.*, 2007). The low-charge saponites give similar values after HDTA modification (Müller *et al.*, 2004). However, the exchanged-Laponite (LAP, ~0.30 charge per half unit cell) does not. This forms a lateral monolayer arrangement of the hydrocarbon tail (Kubies *et al.*, 2002). A second diffraction peak ($38.1-44.1$ Å) (Table 1) occurs in the XRD pattern of HDTA-HecF-0.40 (Fig. 2) and HDTA-HecOH-0.40 (not shown). Although such values are characteristic of a surfactant bilayer structure, IR measurements rule out such an arrangement. It is likely that aggregates of the starting hectorites (not easily powdered) are dispersed more slowly (the dispersions remain white) leading to slower surfactant intercalation (Table 1). This value could correspond to hydrated hectorite ($25-26$ Å) perturbed by the presence of surfactant, while the shorter value accounts for the intercalated surfactant progressively changing its arrangement with the surfactant loading. The last signal is only visible (with the equipment used) when the surfactant loading is >0.75.

A typical ^{13}C CP MAS NMR spectrum is shown in Fig. 3. The attributions are taken from the literature (Kubies *et al.*, 2002), and the signal at ~33 ppm, not visible in previous studies, is tentatively assigned to C_{13} from relaxation measurements (Table 2). The ^{13}C NMR method is currently used to quantify the all-*trans* conformation of long-chain surfactant intercalated in clays (Grandjean, 2006). The ^{13}C CP MAS spectra of the high-charge hectorites (Fig. 3) show two signals at ~34 ppm and ~32 ppm, characteristic of the all-*trans* and *gauche* conformations, respectively. Quantitative analysis (Grandjean, 2006) shows that the all-*trans* conformer
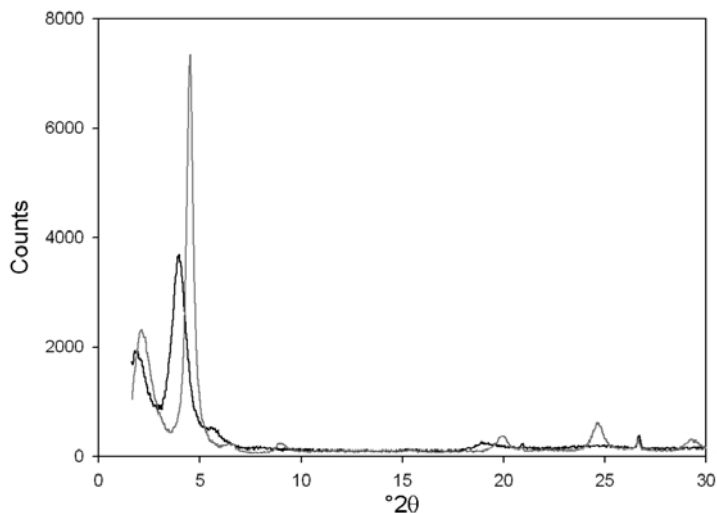
F<small>IG</small>. 2. XRD patterns of HDTA-HecF-0.40. Legend: sample 1 − black; sample 3 − grey. See Table 1 for data.

population of HDTA-HecF-0.80 changes with the amount of intercalated surfactant (62%, 72% and 85% for exchange of 0.36, 0.63 and 0.85 CEC, respectively). Such variation in the conformational ratio is consistent with previous results reported for saponite (Müller *et al.*, 2004) and montmorillonite (He *et al.*, 2004). Accordingly, the all-*trans* conformer of the HDTA-HecF-0.40 (sample 1; Table 1) accounts for 61% of the signal intensity in the 32−34 ppm region. In contrast, the ^{13}C CP NMR spectra of HDTA-HecF-0.40 (samples 2−4, Table 1) and HecOH-0.40 (not shown) with exchange yields <0.7 CEC show a single broad signal at ~33 ppm, which is effectively useless in regard to estimating the conformational ratio. Infrared spectroscopy can be used qualitatively to

F<small>IG</small>. 3. ^{13}C CP MAS NMR spectrum of HDTA-HecF-0.80 (sample C, Table 1).

show the presence of both conformers (Vaia *et al.*, 1994). The IR band of the antisymmetric CH$_2$ stretching mode in the 2917−2929 cm^{-1} range is sensitive to the orientation of the methylene groups, small values characterizing a large content of the all-*trans* ordered state. Accordingly, HDTA-HecF-0.80 (sample B, Table 1) gives rise to a band at 2917 cm^{-1}. In contrast, the three samples HDTA-HecF-0.40 (samples 2−4, Table 1) provide a signal between 2925 and 2927 cm^{-1}. A paraffin-like bilayer structure of the surfactant arrangement is known to generate a large content of all-*trans* conformation (He *et al.*, 2004). Such a surfactant structure in the gallery space of the modified hectorites cannot be correlated with the IR data. The importance of the *gauche* conformation of the hydrocarbon chain probably results from the small surfactant loading of the low-charge hectorites. Variation of the conformational ratio, resulting from the interplay between the repulsive silicate surface-hydrocarbon chain interaction and the interchain van der Waals interaction, has been reported previously for saponites (Müller *et al.*, 2004) and montmorillonites (He *et al.*, 2004).

The ^{23}Na MAS NMR spectrum of the residual Na counter-ions in a partially loaded hectorite shows a broad featureless band, indicating a very asymmetric arrangement of Na ions. For sensitivity reasons, a 2D 3MQMAS NMR experiment was not possible on such samples.

NMR relaxation experiments can be used to probe the dynamics of the intercalated surfactant. The T$_1$
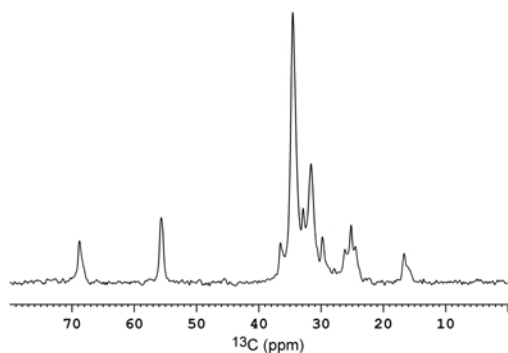
spin-lattice relaxation times in the laboratory frame and $T_{1\rho}$ relaxation times in the rotating frame are sensitive to molecular motions in the MHz and kHz frequency range, respectively. Motional heterogeneity of the surfactant in the clay galleries, including mobility in the MHz and kHz frequency ranges, is observed for the exchanged hectorites, as reported previously for other systems (Mirau *et al.*, 2005; Urbanczyk *et al.*, 2006). The plot of these relaxation times as a function of the correlation time (inversely proportional to temperature) is typically described by a curve with a trough (i.e. the relaxation time decreases initially, before increasing as a function of the correlation time). Accordingly, the plot of the ^{13}C relaxation time in the rotating frame ($T_{1\rho}$(C)) as a function of the carbon position along the surfactant alkyl chain (Fig. 4), indicates mobility enhancement along the chain from N^+-CH_2 (long correlation time) to the terminal methyl group (short correlation time). At greater surfactant loadings, the N^+-CH_2 group (less mobile) shows the smallest ($T_{1\rho}$(C)) value (Table 2), shifting near the minimum value of the curve (Fig. 4). Thus, greater surfactant loading leads to mobility enhancement. Such an observation has been made recently with exchanged-montmorillonites in which greater surfactant loading results in mobility enhancement of the surfactant methyl groups (Wen *et al.*, 2006). In their study on dodecyltrimethylammonium-exchanged clay, those authors note the remarkable mobility of the N^+-CH_3, greater than that of the terminal methyl group. Their conclusions are deduced from the dipolar relaxation time (T_{CH}), which increases with mobility, and greater values are obtained for the methyl head than for the terminal methyl group
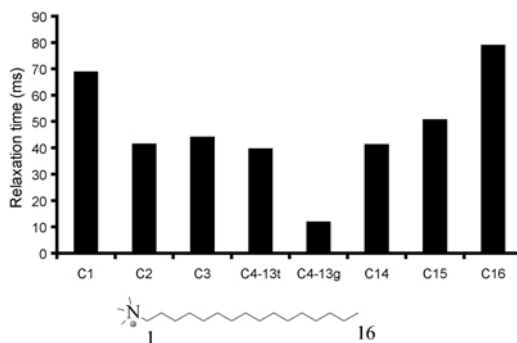

FIG. 4. Plot of the ^{13}C NMR relaxation time in the rotating frame $T_{1\rho}$(C) (ms) as a function of the position along the long hydrocarbon chain (Scheme) of the intercalated surfactant (sample C, Table 1). The correlation time increases (mobility decreases) from right to left.

(Wen *et al.*, 2006). This relaxation time, associated with the $H-^{13}$C dipolar interaction, is averaged on the three bonds of the methyl group. A similar observation was made in previous studies of HDTA-saponites (Hrobarikova *et al.*, 2004), and here (data not shown). However, the opposite effect is deduced from the $T_{1\rho}$(C) values (Table 2). These opposing results can be understood if the complexity of the real situation is considered. The molecular mobility of the inserted surfactant is heterogeneous (Mirau *et al.*, 2005; Urbanczyk *et al.*, 2006) leading to a correlation-time distribution. Accordingly, the measured relaxation times are only mean values of the orientational heterogeneity and precise conclusions cannot be obtained without more detailed theoretical models. These two mean parameters

TABLE 2. Typical ^{13}C relaxation times in the rotating frame $T_{1\rho}$(C) (ms) of the surfactant-exchanged clays.

Nucleus (ppm)	HDTA-HecF-0.80 (C)	HDTA-HecF-0.80 (A)	HDTA-SAP-0.75
C_1 (~69)	68.8	3.73	5.28
C_2 (~29)	41.4	6.21	n.d.
C_3 (~26)	44.1	8.36	9.10
C_{4-12}(t) (~34)	39.6	12.4	12.9
C_{4-12}(g) (~31)	11.9	18.0	17.9
C_{13} (~33)	28.4	13.1	n.d.
C_{14} (~36)	41.2	32.0	n.d.
C_{15} (~24)	50.6	44.1	38.3
C_{16} (~16)	78.9	52.8	48.7
$N-CH_3$ (~55)	57.8	36.6	33.5

n.d.: not detected

(T_{CH}, $T_{1\rho}(C)$), sensitive to motions in the kHz frequency range, may not sample the exact same motions.

Saponite and hectorite are two 2:1 trioctahedral phyllosilicates with cation-isomorphous substitution in the tetrahedral and octahedral layer, respectively. Similar surfactant contents are present in HDTA-HecF-0.80 (A) and HDTA-SAP-0.75 (1.0 CEC). As the $T_{1\rho}(C)$ values are similar and show the same variation in both cases (Table 2), the long-hydrocarbon chain dynamics are not significantly affected by the origin, octahedral or tetrahedral, of the clay negative charge. Such a conclusion is realistic since surfactants with quaternary head groups have no specific ammonium-silicate bonding. However, a different observation is possible with primary ammonium surfactants forming an electrostatic interaction with the silicates (Li & Ishida, 2003; Heinz *et al.*, 2007).

No further information on chain dynamics is obtained from the less-resolved spectra of HDTA-HecF-0.40 (2−4, Table 1).

Finally, we used these modified hectorites to prepare the corresponding poly(ε-caprolactone) (PCL) nanocomposites by *in situ* polymerization (Urbanczyk *et al.*, 2006). The small yields obtained indicate that these modified clays are not appropriate for PCL nanocomposite preparation by this method.

CONCLUSION

In contrast with saponites of variable interlayer charge and high-charge hectorites, the synthetic hectorites of 0.4 charge per half unit cell show partial expansion of the interlayer space when dried at 90ºC and equilibrated at room temperature. Stronger drying conditions are required to eliminate the appropriate XRD signal. The hydroxylated hectorite of 0.4 charge per half unit cell is characterized by two structural ^1H MAS NMR signals near 0 ppm, whereas saponites show a single signal in the same frequency range. The ^{29}Si MAS NMR chemical shifts increase with the hectorite charge, while the ^{23}Na 2D 3QMAS NMR experiments show a larger quadrupolar product for the synthetic hectorites than for the previously studied saponites.

Aggregates of the two low-charge hectorites require longer exchange-time to intercalate significant amounts of surfactant, characterized by a single d_{001} peak. The all-*trans*/*gauche* conformational ratio of the long alkyl chain of the intercalated surfactant changes with the clay charge as observed for modified saponites and montmorillonite. Mobility is heterogeneous, occurring both on the MHz and kHz frequency-scales, increases with the intercalated surfactant content and along the hydrocarbon chain from the polar head to the terminal methyl group. The motional characteristics do not seem to differ from those of the same surfactant intercalated in synthetic saponites. These modified hectorites are not appropriate in the preparation of poly(ε-caprolactone) nanocomposite by *in situ* polymerization.

REFERENCES

Alba M.D., Becerro A.I., Castro M.A. & Perdigón A.C. (2000) High resolution ^1H MAS NMR spectra of 2:1 phyllosilicates. *Chemical Communications*, 37−38.

Amoureux J.-P., Fernandez C. & Steuernagel S. (1996) Z-filtering in MQMAS NMR. *Journal of Magnetic Resonance*, **A123**, 116−118.

Borsacchi S., Geppi M., Ricci L., Ruggeri G. & Veracini C.A. (2007) Interactions at the surface of organophilic-modified laponites: a multinuclear solid-state NMR study. *Langmuir*, **23**, 3953−3960.

d'Espinose de la Caillerie J.-B., Aimeur M.R., El Kortobi Y. & Legrand A.P. (1997) Water adsorption on pyrogenic silica followed by ^1H MAS NMR. *Journal of Colloid and Interface Science*, **194**, 434−439.

Delevoye L., Robert J.-L. & Grandjean J. (2003) ^{23}Na 2D 3QMAS NMR and ^{29}Si, ^{27}Al MAS NMR investigation of Laponite and synthetic saponites of variable interlayer charge. *Clay Minerals*, **38**, 63−69.

Grandjean J. (2006) Solid-state NMR study of modified clays and polymer/clay nanocomposites. *Clay Minerals*, **41**, 567−586.

Hamilton D.L. & Henderson C.M.B. (1968) Preparation of silicate compositions by a gelling method.

Mineralogical Magazine, **36**, 832−838.

He H., Frost R.L., Deng F., Zhu J., Wen X. & Yuan P. (2004) Conformation of surfactant molecules in the interlayer of montmorillonite, studied by ^{13}C MAS NMR. *Clays and Clay Minerals*, **52**, 350−356.

Heinz H., Vaia R.A., Krishnamoorti R. & Farmer B.L. (2007) Self-assembly of alkylammonium chains on montmorillonite: effect of chain length, head group structure and cation exchange capacity. *Chemistry of Materials*, **19**, 59−68.

Hrobarikova J., Robert J.-L., Calberg C., Jérôme R. & Grandjean J. (2004) Solid-state NMR study of intercalated species in poly(ε-caprolactone)/clay nanocomposites. *Langmuir*, **20**, 9828−9833.

Kubies D., Jérôme R. & Grandjean J. (2002) Surfactant molecules intercalated in laponite as studied by ^{13}C and ^{29}Si MAS NMR. *Langmuir*, **18**, 6159−6163.

Lagaly G. (1986) Interaction of alkylamines with different types of layered compounds. *Solid State Ionics*, **22**, 43−51.

Li Y. & Ishida H. (2003) Characterization-dependent conformation of alkyl tail in the nanoconfined space: hexadecyl in the silicates galleries. *Langmuir*, **19**, 2479−2484.

Mirau P.A., Vaia R.A. & Garber J. (2005) NMR characterization of the structure and dynamics of polymer interfaces in clay nanocomposites. *Polymer Preprints*, **46**, 440−441.

Müller R., Hrobarikova J., Calberg C., Jérôme R. & Grandjean J. (2004) Structure and dynamics of cationic surfactants intercalated in synthetic clays. *Langmuir*, **20**, 2982−2985.

Osman M.A., Ploetze M. & Skrabal P. (2004) Structure and properties of alkylammonium monolayers self-assembled on montmorillonite platelets. *Journal of Physical Chemistry*, **B108**, 2580−2588.

Rocha J., Morais C.M. & Fernandez C. (2003) Novel nuclear magnetic resonance techniques for the study of quadrupolar nuclei in clays and other layered materials. *Clay Minerals*, **38**, 259−278.

Sanz J., Robert J.-L., Diaz M. & Sobrados I. (2006) Influence of charge location on ^{29}Si NMR chemical shift of 2:1 phyllosilicates. *American Mineralogist*, **91**, 544−550.

Urbanczyk L., Hrobarikova J., Robert J.-L., Calberg C., Jérôme R. & Grandjean J. (2006) Motional hetero-geneity of intercalated species in modified clays and poly(caprolactone)/clay nanocomposites. *Langmuir*, **22**, 4818−4824.

Vaia R.A., Teukolsky R.K. & Giannelis E.P. (1994) Interlayer structure and molecular environment of alkylammonium layered silicates. *Chemistry of Materials*, **6**, 1017−1022.

Wen X., He H., Zhu J., Jun Y., Ye C. & Deng F. (2006) Arrangement, conformation, and mobility of surfac-tant molecules intercalated in montmorillonite pre-pared at different pillaring reagent concentrations as studied by solid-state NMR spectroscopy. *Journal of Colloid and Interface Science*, **299**, 754−760.